

# Mitochondrial Proteomics and Transcriptional Analysis of Cytoplasmic Male Sterility in Sugar Beet using iTRAQ and qRT-PCR

Tianjiao Liu (✉ [sfangelos@163.com](mailto:sfangelos@163.com))

Harbin Institute of Technology School of Chemistry and Chemical Engineering <https://orcid.org/0000-0001-5048-3352>

Dayou Cheng

Harbin Institute of Technology School of Chemistry and Chemical Engineering

Xue Han

Harbin Institute of Technology School of Chemistry and Chemical Engineering

Jie Cui

Harbin Institute of Technology School of Chemistry and Chemical Engineering

Cuihong Dai

Harbin Institute of Technology School of Chemistry and Chemical Engineering

Junliang Li

Wenzhou University

Naiguo Liang

Huaiyin Institute of Technology

---

## Research Article

**Keywords:** Sugar beet, CMS, Mitochondrion, Proteomics, iTRAQ, qRT-PCR

**Posted Date:** January 6th, 2022

**DOI:** <https://doi.org/10.21203/rs.3.rs-1120889/v1>

**License:** © ⓘ This work is licensed under a Creative Commons Attribution 4.0 International License.

[Read Full License](#)

---

# Abstract

Sugar beet (*Beta vulgaris* L.) is an important raw material for the sugar industry, and its output is second only to sugar cane. Cytoplasmic male sterility (CMS) is a phenomenon of pollen abortion that has important implications in sugar beet hybrid breeding. Male plant sterility is usually considered to be associated with mitochondrial dysfunction. Although mitochondrial genes associated with male sterility have been well explored, the different mitochondrial proteomics of CMS in sugar beet are still poorly understood. In this study, differentially expressed mitochondrial proteomic analysis was performed on the flower buds of the male sterile line (DY5-CMS), its maintainer line (DY5-O) and a fertility restorer line (CL6), using an isobaric tag for relative and absolute quantitation (iTRAQ) technology. A total of 2260 proteins were identified by mass spectrometry, of which 538 were differentially expressed proteins. Most of them were involved in protein metabolism, carbohydrate and energy metabolism, and binding. More specifically, some cysteine and methionine metabolism proteins (A0A0J8BGE0, A0A0J8CZM6, A0A0J8D7W0 and A0A0J8BCR7) may play important roles during the formation of CMS. This study provided an in-depth understanding of the CMS molecular mechanism at the protein level in sugar beet.

## 1. Introduction

Cytoplasmic male sterility (CMS) is a maternally inherited condition in which higher plants fail to produce functional pollen but maintain female fertility [1]. CMS is a useful trait for commercial hybrid breeding because inactive pollen eliminates the need for the expensive process of stamen removal [2]. CMS has been reported in over 150 plant species and is often associated with chimeric mitochondrial open reading frames (ORFs) [3–4]. A variety of key events focus on mitochondria, including oxidative phosphorylation and programmed cell death (PCD). In many cases, transcripts originating from these altered mitochondrial ORFs are translated into proteins that have been identified in many crops and appear to interfere with pollen development and mitochondrial function [5]. It has been demonstrated that these mitochondrial proteins are associated with CMS [5] and co-segregated with the sterility phenotype [6]. Nuclear genes (Rf) that restore the fertility of the male-sterile cytoplasm prevent the deleterious effects of mitochondrial abnormalities, and reduce the amount of sterility-related proteins [5–7].

Sugar beet (*Beta vulgaris* L.) is an important raw material for the sugar industry and a potential source of alternative energy [8]. CMS in sugar beets was first discovered by F.V. Owen [9], and the so-called Owen cytoplasm has subsequently been used worldwide for hybrid seed production. The complete nucleotide sequences of the mitochondrial genomes from fertile and Owen CMS beets have been determined [10–11], which allows the in-depth study of the protein products of these mitochondrial genomes. Structural differences in the mitochondrial loci of *atp1*, *atp6*, *cob*, *cox1*, *cox2* and *rps3* have been found in the comparison of sugar beet CMS and fertile lines [12–15]. Four transcribed open reading frames (ORFs) of *Satp6*, *Scox2-2*, *Sorf324* and *Sorf119*, which may produce novel proteins that affect mitochondrial function in pollen-producing tissues, have also been identified [11, 16]. It was reported that polypeptides of 6 kDa, 10 kDa, 35 kDa and 12 kDa may be associated with the expression of CMS in sugar beet [7, 16–17], and the decreased activity of complex V and the increase of other complexes with ATPase activity

may affect CMS in sugar beet [18]. However, these findings are not enough to explore the secrets of beet CMS systems. A large number of CMS-associated mitochondrial proteins have been identified and described in rice [2, 19], wheat [20–21], maize [22–23], brassica [1, 24], tomato [25] etc. However, no two CMS mutations described to date are identical [6]. Sugar beet, as a complex glycophytic member of Chenopodiaceae, is different from other plants. Little is known about the mitochondrial proteins involved in the expression of the CMS phenotype in sugar beet, and the molecular mechanism that these proteins cause remains an enigma.

Although the molecular mechanisms of CMS have been extensively investigated, there is little information on quantitative comparisons of mitochondrial proteomics in fertile and CMS beet lines, especially with reference to differentially expressed proteins (DEPs) and metabolic pathways. In this study, a comprehensive analysis of mitochondrial proteomics and transcription of the CMS phenotype in sugar beet was performed by using an isobaric tag for relative and absolute quantitation (iTRAQ) technology and quantitative real-time PCR (qRT-PCR). More mitochondrial proteins associated with CMS beets were found through mass spectrometry analysis, and the reliability of the results was further verified by quantitative analysis of the genes. The molecular function of these proteins, as well as the metabolic pathways involved, are described in detail. Possible interactions among these proteins are also discussed. This report thus provides the general characteristics of the CMS-associated mitochondrial proteome in beets. The candidate protein and metabolic pathway provided in this report would be conducive to revealing the molecular mechanism of CMS in beets.

## 2. Materials And Methods

### 2.1. Plant materials

Three lines of sugar beet (*Beta vulgaris* L.) were used in this study, including the male-sterile line DY5-CMS, maintainer line DY5-O and fertility-restored line CL6. The DY5 pair is composed of two lines that have the same genetic background through repeated backcrossing, but their cytoplasmic genomes are different. CL6 is the continuous system selection offspring of GW-65 in the 1960s (in the USA). Three biological replicates of all the materials were sampled during the vegetative growth stage. These replicates were mixed to create sample pools for subsequent experiments.

### 2.2. Extraction and quantification of mitochondrial proteins

Mitochondria were isolated from 20 g of sugar beet roots using the Plant Mitochondrial Extraction Kit (BestBio, Shanghai, China). The principle of the kit is that mechanical shear force is used to destroy the cell wall and cell membrane and release organelles, and then, based on the difference in the sedimentation coefficient of organelles, mitochondria are separated using differential centrifugation combined with density gradient centrifugation. According to previous studies, this is an improved optimization method [26–30]. Ensuring the quality of mitochondria isolated from test material is a key step in proteomics. Janus Green B is a vital stain used for the identification of mitochondria, which binds to cytochrome c oxidase to give a blue–green color [20, 21, 31]. The isolated mitochondria were stained

with 0.5% Janus Green B (Solarbio, Beijing, China) for 1–3 min, and their activity was observed under an optical microscope (COIC, Chongqing, China). Scanning electron microscopy (SEM; Hitachi SU8010, Tokyo, Japan) of frozen samples was used to examine mitochondrial integrity. Mitochondria extracted from 20 g of beet roots were dissolved in 5 mL of SDT buffer (4% SDS, 100 mM DTT and 150 mM Tris-HCl, pH 8.0). The suspension was incubated in boiling water for 30 min followed by ultrasonication (80 W, 10 s ultrasonication at a time, every 15 s, for 10 times) [32]. The supernatant obtained after centrifugation (25°C, 14000 × g, 45 min) contained mitochondrial proteins, and the protein concentration was determined following the manufacturer's protocol (BCA Protein Assay Reagent, Promega, USA).

## 2.3. iTRAQ labeling and strong cation exchange fractionation

Briefly, 100 µg mitochondrial proteins from each sample was digested by trypsin (37°C, 16–18 h), and the peptides were quantified by OD280. Peptides (80 µg) from each sample were labeled with the iTRAQ Reagent-8plex Multiplex Kit (Applied Biosystems, Foster, CA, USA). The samples were labeled CL6-113, DY5-O-114 and DY5-CMS-115. All the labeled samples were mixed and subjected to strong cation exchange fractionation by using an AKTA Purifier 100 (GE Healthcare, Chicago, IL, USA) and a polysulfoethyl (4.6 × 100 mm) column (5 µm, 200 Å) (PolyLCInc, Columbia, MO, USA). The fractions obtained were dried under vacuum and desalted using a C18 cartridge (Sigma–Aldrich, St. Louis, MO, USA).

## 2.4. LC–MS/MS

The peptide fractions obtained were subjected to high-performance liquid chromatography (HPLC) with an Easy nLC 1000 system (Thermo Fisher Scientific, Waltham, MA, USA). Solvents were composed of formic acid:acetonitrile:water (A: 0.1:0:99.9%; B:0.1:84:15.9% 1v/v). The samples were loaded onto Thermo Scientific EASY columns (2 cm × 100 µm × 5 µm-C18 and 75 µm × 100 mm × 3 µm-C18) for analytical separation at a flow rate of 300 nL min<sup>-1</sup> for 60 min. The gradients used were as follows: 0–50 min, B from 0–40%; 50–57 min B from 40–100%; 57–60 min, B maintained at 100%. Data were acquired using a Thermo Q-Exactive mass spectrometer (Thermo Fisher Scientific) and the experimental procedure was conducted according to a previous method [33]. Mass spectrometry (MS) data were chosen for higher-energy collisional dissociation (HCD) fragmentation from the most abundant precursor ions detected in the survey scan (300–1800 m/z). Determination of the target value was based on predictive automatic gain control (pAGC). Dynamic exclusion duration was 40 s. Survey scans were acquired at a resolution of 70,000 at m/z 200, and a resolution of 17,500 at m/z 200 was set for HCD spectra. The normalized collision energy was 30 eV and the underfill ratio was defined as 0.1%.

Data were processed using Mascot 2.2 and Proteome Discoverer 1.4 (Thermo Fisher Scientific), and compared with the Uniprot-beta-Vulgaris-29810-20170309.fasta database (28910 sequences, download on 2017-03-09, [http://www.uniprot.org/uniprot/?query="beta+vulgaris"&sort=score](http://www.uniprot.org/uniprot/?query=)). The parameters used in Mascot searches for normal peptides were according to the description in Hu et al. (2015) [33]: Enzyme: Trypsin, max missed cleavage: 2, Fixed modification: Carbamidomethyl (C), iTRAQ4plex (K),

iTRAQ4plex (N-term), Variable modification: Oxidation (M), Peptide mass tolerance: 20 ppm, MS/MS tolerance: 0.1 Da. Protein identification was calculated by only unique peptides, and the normalization method and protein change ratio type (up- or downregulated) were both set as medians. The results were filtered based on a false discovery rate (FDR) of no more than 1% to guarantee the result's confidence [34] and a Mascot probability of 95%. When the abundance level of a protein showed a difference corresponding to a 1.3-fold or 0.77-fold change from DY5-CMS/DY5-O, DY5-CMS/CL6, and CL6/DY5-O comparisons, and had a statistically significant level (P value<0.05) by significance A analysis, the protein was then considered to be a differentially expressed protein (DEP).

## 2.5. Bioinformatics

Functional analysis and pathway analysis of proteins were performed using GO (<http://www.geneontology.org/>) and KEGG (<http://www.kegg.jp/kegg/kaas/>), respectively. Protein–protein interaction networks were constructed using the publicly available program STRING (<http://string-db.org/>). STRING, a database of known and predicted protein–protein interactions, quantitatively integrates the interaction data (from four sources: the genomic context, high-throughput experiments, coexpression and previous knowledge) for a large number of organisms and transfers information between these organisms under applicable conditions [33].

For statistical analysis, Fisher's exact test with the hypergeometric algorithm was used to calculate P values, and the cutoff of P values lower than 0.05 was set to select significantly enriched terms in categories. FDR attained by the Benjamini-Hochberg method was used to adjust P values.

## 2.6. qRT–PCR

We performed qRT–PCR to verify whether the iTRAQ results were consistent with the quantitative results of genes in the roots and leaves. Total RNA was extracted from the roots and leaves of sugar beet with a TaKaRa MiniBEST Plant RNA Extraction Kit (Takara Bio, Osaka, Japan), and subjected to first-strand cDNA synthesis using a PrimeScript™ RT reagent kit (Takara Bio) according to the manufacturer's instructions. Ct values were obtained via the real-time fluorescence detection method with SYBR® Premix EX Taq™ II (Takara Bio) on an ABI 7300 Real Time PCR System (Applied Biosystems). The primers used were designed according to the cDNA sequences published on NCBI by using Primer-BLAST (<https://www.ncbi.nlm.nih.gov/tools/primer-blast/>; Table 1). The *BvICDH* gene (GenBank AF173666) was selected as a reference gene as described previously [35]. The  $2^{-\Delta\Delta CT}$  method, SPSS 19.0 software, and Origin 8.0 software were used for statistical analysis and mapping. All reactions were performed in three biological and three technical replicates.

Table 1  
Sequences of the primers used for qRT-PCR.

Accession	5'–3' sequence (F)	5'–3' sequence (R)
<i>BvICDH</i>	cacaccagatgaaggccgt	ccctgaagaccgtgccat
<i>Cu/Zn-SOD</i>	catgtgggtgacctgggaaa	ggatcagcatgcaccacaac
<i>Gsh2</i>	ttcccagcgcttctggttaag	gagacctctgctccgcatcaa
<i>CHI2-A</i>	agtaagggaccgtttggcag	cgatctcagctgtgcctgaa
<i>ATP-α</i>	ggggattaccggcttttga	ggcagccggtagaagaaact
<i>GAPDH</i>	actggtgctgatttgcgctg	ggcttttgggtagccgtga
<i>CS</i>	ctcgagttggccagcaatca	accggatacccttcttctggg
<i>H2A</i>	acgtgttggtactggtgctc	cgttcctcacagcaaggaga
<i>AAT</i>	aactggttctctccgccttg	ctcggacatggaactctgg
<i>SHMT</i>	acatgctgacggaagcagtt	ccattgtctggccttctcgt
<i>PGDH</i>	gcccctcaatcttggctcc	gtcccgctccttacgatcag
<i>L36</i>	atcgcaaagggaaaaccagc	atctcctcctccagcagacc
<i>GS</i>	cggagaaggaaggcaaaggt	ctcagcttcgagtgtgggtt
<i>Annexin</i>	ggatcctcctgagcgtgatg	tgtgtgttaacctctggccc

## 3. Results

### 3.1. Isolation of mitochondria from sugar beet

The isolated mitochondria were morphologically intact, and spherical-ellipsoidal in shape (Supplementary Fig. S1).

### 3.2. iTRAQ analysis of DEPs

In this study, a total of 2260 proteins were identified in the lines DY5-O, DY5-CMS and CL6 at an FDR of 1%. The full list of these proteins is available in Supplementary Table S1. In detail, proteins with a minimum fold change of  $\pm 1.3$  or greater in abundance, FDR  $< 0.01$  and  $P < 0.05$ , were regarded as DEPs because iTRAQ quantification estimated the real amount of fold change from DY5-CMS/DY5-O, DY5-CMS/CL6, and CL6/DY5-O comparisons. Based on this criterion, 538 DEPs from DY5-CMS/DY5-O, DY5-CMS/CL6, and CL6/DY5-O comparisons were selected for further analysis (Fig. 1 and Supplementary Table S2), including 191 DEPs (106 upregulated and 85 downregulated) between DY5-CMS and DY5-O, 190 DEPs (111 upregulated and 79 downregulated) between DY5-CMS and CL6, and 157 DEPs (76 upregulated and 81 downregulated) between CL6 and DY5-O.

The two proteins present at the highest concentration in DY5-CMS compared to DY5-O were citrate synthase and 60S ribosomal protein L7-2 which had fold change values of 3.725 and 5.883, respectively. Interestingly, 60S ribosomal protein L17-2 and citrate synthase were also found to be higher in DY5-CMS than in CL6, with over 1.5-fold change values. In contrast, 65 and 58 kinds of proteins were downregulated in DY5-CMS compared to DY5-O and CL6, respectively. In addition, LysM domain-containing GPI-anchored protein 2 was the protein present at the highest concentration in CL6 compared to DY5-O and DY5-CMS, with fold change values of 8.337 and 6.849, respectively. DEPs that differentiate DY5-CMS from DY5-O and CL6 in the same way are summarized in Table 2.

Table 2  
DEPs that differentiate DY5-CMS from DY5-O and CL6 in the same way

Accession	Description	DY5-CMS/DY5-O		DY5-CMS/CL6	
		Fold change	Significance A	Fold change	Significance A
A0A0J8BGE0	Aspartate aminotransferase	1.452	0.0163534	1.620	0.00757495
A0A0J8BI86	Citrate synthase	3.725	3.84002E-17	1.706	0.00310876
A0A023ZQE9	Ribosomal protein	1.811	0.000137893	1.747	0.0020135
A0A023ZRD6	Ribosomal protein L14	2.021	6.40422E-06	1.627	0.00705329
A0A0J8B5C0	Ribosomal protein L2	1.619	0.00196023	1.767	0.00162577
A0A0J8BD62	50S ribosomal protein L12	1.819	0.000123001	1.483	0.0291581
A0A0J8BIC4	50S ribosomal protein L3	2.435	1.17916E-08	1.635	0.00649925
A0A0J8C2D9	60S ribosomal protein L12-1	1.628	0.00173858	1.729	0.00243823
A0A0J8C9Y6	60S ribosomal protein L7-2	5.883	8.67828E-30	1.590	0.0102588
A0A0J8CGP6	60S ribosomal protein L17-2	1.463	0.0143202	1.457	0.0372117
A0A0J8EC56	3-isopropylmalate dehydrogenase	1.429	0.0215072	1.452	0.0389793
A0A0J8B804	Ent-kaurene oxidase	1.486	0.010811	1.835	0.000778662
A0A0J8BCR7	Glutamate-cysteine ligase	1.370	0.0423887	1.622	0.00742225
A0A0J8BH48	Peptide-N4-(N-acetyl-beta-glucosaminy) asparagine amidase A	1.814	0.000132112	1.602	0.00909132
A0A0J8BT32	EG45-like domain containing protein	1.529	0.00631564	1.602	0.00909132
A0A0J8CBL4	Mannose/Glucose-specific lectin	1.684	0.0008152	1.856	0.000618751
A0A0J8CL98	Putative BPI/LBP family protein At1g04970	1.469	0.0133136	1.497	0.0255256
A0A0J8CUD8	Peptidyl-prolyl cis-trans isomerase	1.487	0.0106785	1.665	0.00477079
A0A0J8CWP4	D-amino-acid transaminase	2.054	3.91164E-06	1.643	0.00598709
A0A0J8CZA0	Probable L-type lectin-domain containing receptor kinase S.5	1.593	0.0027643	1.476	0.0311499
A0A0J8D7U9	Syntaxin-71 isoform X2	1.534	0.00592728	1.522	0.0200702

Accession	Description	DY5-CMS/DY5-O		DY5-CMS/CL6	
		Fold change	Significance A	Fold change	Significance A
A0A0J8EP18	GDSL esterase/lipase 5	3.126	2.91918E-13	2.379	1.6068E-06
A0A0J8FK42	Probable enoyl-CoA hydratase 1	1.787	0.000193991	1.476	0.0311499
P55232	Glucose-1-phosphateadenylyl transferase small subunit	1.581	0.00323466	2.080	5.03507E-05
A0A0J8C5G7	Annexin	0.658	0.0119996	0.598	0.0114524
A0A0J8B3V8	Protein phosphatase 2C 70	0.523	9.60623E-05	0.535	0.00209757
A0A0J8BHH6	Glycine-rich RNA-binding protein	0.709	0.0393164	0.590	0.0094641
A0A0J8BIB6	Late embryogenesis abundant protein Dc3	0.266	1.37639E-15	0.558	0.00411701
A0A0J8BK22	Glycine-rich RNA-binding protein 7	0.672	0.0170848	0.583	0.00796584
A0A0J8C889	Formin-like protein	0.502	3.35277E-05	0.528	0.00168471
A0A0J8CFP7	Pyruvate decarboxylase 2	0.523	9.60623E-05	0.567	0.00526482
A0A0J8CLI0	Basic proline-rich protein isoform X1	0.646	0.0087051	0.609	0.0147303
A0A0J8D4W8	Cinnamoyl-CoA reductase 2 isoform X1	0.559	0.000468944	0.539	0.0023703
A0A0J8D7W0	Cysteine synthase	1.413	0.0259439	1.519	0.0206616
A0A0J8CZM6	Aspartate aminotransferase	1.374	0.0405303	1.598	0.00946563

### 3.3. Gene ontology analysis of DEPs

The DEPs associated with CMS were annotated using Gene Ontology (GO) according to the cell component and biological and molecular function (Supplementary Fig. S2 and Supplementary Table S3-1). Concerning biological processes, the DEPs from the DY5-CMS/DY5-O, DY5-CMS/CL6 and CL6/DY5-O comparisons were classified into 8, 11 and 10 categories, respectively. The top categories with the highest number of DEPs from these three comparisons were metabolic processes (90 in DY5-CMS/DY5-O, 78 in DY5-CMS/CL6 and 63 in CL6/DY5-O), cellular processes (59 in DY5-CMS/DY5-O, 65 in DY5-CMS/CL6 and 46 in CL6/DY5-O) and single organism processes (44 in DY5-CMS/DY5-O, 43 in DY5-CMS/CL6 and 37 in CL6/DY5-O), indicating that these three biological processes were the most important in sugar beet under CMS conditions. The DEPs from these three comparisons were also involved in cellular component organization or biogenesis, response to stimulus, biological regulation and

localization. More specifically, a small number of DEPs from the DY5-CMS/DY5-O and DY5-CMS/CL6 comparisons were involved in the negative regulation of biological processes, and the DEPs from the DY5-CMS/CL6 and CL6/DY5-O comparisons were involved in multiorganism and immune system processes. Furthermore, only the DEPs between DY5-CMS and CL6 were involved in reproduction, whereas those from CL6/DY5-O participated in signaling. Concerning the cell component, 125, 131 and 76 proteins were annotated in the DY5-CMS/DY5-O, DY5-CMS/CL6 and CL6/DY5-O comparisons, respectively, showing an unbiased distribution in different compartments and free from contaminating thylakoid membranes. Concerning the molecular function, the DEPs from the DY5-CMS/DY5-O, DY5-CMS/CL6 and CL6/DY5-O comparisons were classified into 7, 6 and 8 categories, respectively. The top 2 categories with the highest number of DEPs from these three comparisons were binding (56 in DY5-CMS/DY5-O, 66 in DY5-CMS/CL6 and 55 in CL6/DY5-O) and catalytic activity (69 in DY5-CMS/DY5-O, 59 in DY5-CMS/CL6 and 54 in CL6/DY5-O), indicating that both functional categories were the most important in sugar beet under CMS conditions.

### 3.4. Pathway analysis of DEPs

To further address the functional consequences of DEPs associated with CMS, pathway analysis based on KEGG was conducted. According to the KEGG results, signaling pathways related to CMS with significant expression level changes in the comparisons. DY5-CMS/DY5-O, DY5-CMS/CL6 and CL6/DY5-O were classified into 22, 11 and 9 categories, respectively (Fig. 2 and Supplementary Table S3-2). The DEPs were more enriched in metabolic pathways (22.49%); biosynthesis of secondary metabolites (14.79%); biosynthesis of amino acids (8.28%); ribosome (7.69%); carbon metabolism (6.51%); cysteine and methionine metabolism (4.14%); arginine biosynthesis (3.55%); valine, leucine and isoleucine degradation (3.55%); 2-oxocarboxylic acid metabolism (3.55%); amino sugar and nucleotide sugar metabolism (2.96%); alanine, aspartate and glutamate metabolism (2.96%); phenylalanine, tyrosine and tryptophan biosynthesis (2.37%); arginine and proline metabolism (2.37%); glycine, serine and threonine metabolism (2.37%); and flavonoid biosynthesis (1.78%). For the DY5-CMS/CL6 comparison, the DEPs were more enriched in ribosome (20.00%); biosynthesis of amino acids (18.18%); carbon metabolism (14.55%); 2-oxocarboxylic acid metabolism (9.09%); cysteine and methionine metabolism (9.09%); carbon fixation in photosynthetic organisms (7.27%); arginine biosynthesis (5.45%); and alanine, aspartate and glutamate metabolism (5.45%). Last, for the CL6/DY5-O comparison, the DEPs were mainly related to the biosynthesis of amino acids (22.22%); carbon metabolism (22.22%); aminoacyl-tRNA biosynthesis (11.11%); glycolysis/gluconeogenesis (11.11%); flavonoid biosynthesis (8.33%); valine, leucine and isoleucine degradation (8.33%); nitrogen metabolism (5.56%); and arginine biosynthesis (5.56%).

The four metabolic pathways in the three comparisons all included the biosynthesis of amino acids; carbon metabolism; valine, leucine and isoleucine degradation; and arginine biosynthesis. In particular, 5 metabolic pathways, including ribosome; 2-oxocarboxylic acid metabolism; alanine, aspartate and glutamate metabolism; tropane, piperidine and pyridine alkaloid biosynthesis; and isoquinoline alkaloid biosynthesis, were only found in the DY5-CMS/DY5-O and DY5-CMS/CL6 comparisons. However, flavonoid biosynthesis was only found in the DY5-CMS/DY5-O and CL6/DY5-O comparisons. These

pathways are involved in carbohydrate and energy metabolism, protein metabolism, the biosynthesis of secondary metabolites and nucleotide metabolism, which means that these pathways were the most important in sugar beet under CMS conditions.

### 3.5. Network analysis of DEPs

To better understand how sugar beet transmits CMS signaling through protein–protein interactions, the DEPs associated with CMS were analyzed by STRING. This analysis revealed a protein association network that has a very notable interaction (Fig. 3). According to the protein association network (Fig. 3), the DEPs were highly enriched in carbon metabolism, metabolism of amino acids and ribosomes. Abbreviations of the specific protein names in the network are given in Supplementary Table S3-3. These pathways are involved in carbohydrate and energy metabolism, protein metabolism and nucleotide metabolism. Interestingly, 5 DEPs occupied the key regulatory sites of this protein network, including serine hydroxymethyltransferase (SHMT), D-3-phosphoglycerate dehydrogenase (PGDH), glyceraldehyde-3-phosphate dehydrogenase (GAPDH), aspartate aminotransferase (AAT) and citrate synthase (CS) (Fig. 3). Among these proteins, only AAT is involved in protein metabolism, and the rest are involved in carbohydrate and energy metabolism.

### 3.6. Gene expression analysis of specific DEPs

qRT–PCR analysis was performed to investigate gene expression changes at the mRNA level, and thirteen genes were selected for this analysis (Fig. 4). The genes analyzed in the roots were different from those in the leaves based on the pattern of changes at the mRNA level. Furthermore, on the basis of the pattern of changes at the protein and mRNA levels, the genes analyzed in the roots were clustered into three groups: Group I, consistent changes at the transcript and protein levels; group II, inverse changes at the transcript and protein levels; and group III, changes only at the protein level. More specifically, five genes, *chalcone-flavanone isomerase family protein (CHI 2-A)*, *ATP synthase subunit  $\alpha$  (ATP- $\alpha$ )*, *CS*, *PGDH* and *glutamine synthetase (GS)*, were clustered in Group I; seven genes, *glutathione synthetase (GSH-S)*, *GAPDH*, *histone 2A (H2A)*, *AAT*, *SHMT*, *60S ribosomal protein L36 (L36)* and *annexin*, were clustered in group II; and only *Cu/Zn-superoxide dismutase (Cu/Zn-SOD)* was clustered in group III.

## 4. Discussion

Cytoplasmic male sterility (CMS) is a complex phenomenon of the abnormal development of stamens and pollen in flowering plants and involves the interaction of nuclear and cytoplasmic genes, a variety of metabolic processes and structural changes [24]. A mitochondrial proteomics study on CMS of sugar beet has previously been reported [18], but gel-based methods limited the detection of proteins. iTRAQ technology, as a nongel-based quantitative proteomics approach, has been used in research on the male sterility of some plants due to its unique advantages [36–37], but to date, there is no related report on CMS in sugar beet. To further elucidate the molecular mechanism of CMS in sugar beet, a comparative mitochondrial proteomic analysis was performed on the CMS line DY5-CMS, its maintainer line DY5-O and the restorer line CL6 using iTRAQ and qRT–PCR. By using iTRAQ technology, we identified a large

number of DEPs that were either up- or downregulated in CMS beet relative to the other lines. The possible potential effects of some DEPs and metabolic pathways on male sterility in sugar beet are discussed below.

## 4.1. DEPs involved in protein metabolism

Proteins perform physiological functions and play essential roles in the growth and development of organisms by interacting with other molecules. Our understanding of CMS in beets was advanced by proteins involved in protein metabolism that included cysteine and methionine metabolism, nitrogen metabolism and ribosomes. In this study, cysteine and methionine metabolism proteins AAT (A0A0J8BGE0), AAT (A0A0J8CZM6), GCL (A0A0J8BCR7) and Cs (A0A0J8D7W0) were more accumulated in the CMS line than in the maintainer and restorer lines (Table 2 and Fig. 5). In contrast, GSH-S (A0A0J8FCL3) was downregulated in the CMS line compared to the restorer line (Supplementary Table S2). AAT is an important enzyme in amino acid metabolism that catalyzes the reversible transfer of an  $\alpha$ -amino group between aspartate and glutamate [38]. A previous study of AAL toxin-induced cell death in *Arabidopsis thaliana* indicated that AAT was included in the most upregulated genes 24 h after AAL treatment [39]. This result suggested that AAT was a potentially important gene for PCD and played a role in the activation of cell death. In humans and other animals, AAT has long been used as an established serum marker for cardiac and liver damage and may also be hypothesized as a useful indicator of cell death [40]. PCD, as an active suicidal process, is an essential part of many developmental processes and responses to plant pathogens [41–42]. The results from a previous study also indicated that the PCD process induced by oxidative stress may be the physiological cause for the abortion of microspores in the maize CMS-C line [21]. In addition, GCL is the rate-limiting enzyme in the GSH biosynthesis pathway [43]. GSH is an antioxidant and eliminates free radicals, and strains lacking glutathione have been reported to be susceptible to oxidative stress induced by toxins of peroxide and superoxide anions and lipid hydroperoxides [44–45]. Elevated GCL in the CMS line may limit the GSH biological pathway, which cannot normally participate in cellular protection by hindering the scavenging of free radicals and enzymatic reduction reactions. This finding was also supported by the downregulation of GSH-S in the CMS line. The abundance changes of GSH-S may have broken the process of response to stimulus and even be a key factor in CMS, and explanations for this could be: (i) Insufficient GSH-S might inhibit glutathione synthesis, which may reduce the ability of free radical scavengers in CMS line and cause an improper function in plant defense and stress tolerance; (ii) The level of ROS as a toxin is elevated due to the downregulation of GSH-S, which may be involved in the PCD process. In contrast, Cs was defined as a sensor whose activity is balanced between cysteine consumption and sulfate assimilation and controls cysteine syntheses within the cell [46]. As KEGG results of cysteine and methionine metabolism (bvg00270) show (Fig. 5), cysteine is converted from serine (via acetylserine) by the transfer of hydrogen sulfide in plants. Interestingly, elevated cysteine is used as the sulfur donor for GSH synthesis [46], while GSH-S was downregulated in this study. Previous research also shows that Cs catalyzes the biosynthesis of cysteine on the basis of a regulatory network,

which mediates between inorganic sulfur supply and the demand for reduced sulfur during plant growth and in response to environmental changes [47–48].

In this study, GS (A0A0J8BRK7) was downregulated in the CMS line compared to the maintainer line, and this effect was reversed upon fertility restoration (Supplementary Table S2). These findings were validated by qRT–PCR analysis (Fig. 3). GS is one of the key enzymes of nitrogen metabolism and catalyzes the synthesis of glutamine with  $\text{NH}_4^+$  and glutamic acid as substrates [49]. GS plays a central role in maintaining the balance of carbon and nitrogen, such as preventing toxins generated by excessive  $\text{NH}_4^+$  [49]. Therefore, the synthesis of glutamine may be inhibited by the downregulation of GS in CMS beets, which disrupts the balance between carbon and nitrogen. CMS may be caused by toxins generated by excessive  $\text{NH}_4^+$ . Consistent with our results, GS was also downregulated or absent in sterile lines of pepper and wolfberry, which affected amino acid metabolism and cytoskeleton biosynthesis, thereby inducing male sterility [50–51]. Many ribosomal proteins that differentiate DY5-CMS from DY5-O and CL6 in the same way were also found in this study (Table 2). They are major components of ribosomes and play important roles in protein synthesis.

In many species, a large number of DEPs involved in protein metabolism were identified, which confirmed that this pathway was associated with CMS [20, 21, 24, 25, 31, 36 and 37]. According to the results in Table 2, cysteine and methionine metabolism was preferentially upregulated under CMS conditions. There were more products of protein metabolism in the CMS line than in the maintainer and restorer lines (Table 2 and Supplementary Table S2-1).

## 4.2. DEPs involved in carbohydrate and energy metabolism

The main physiological function of carbohydrate and energy metabolism is to provide energy and a carbon source. Some proteins affected include GAPDH (A3FMH0), ATP- $\alpha$  (Q9XPH4), SHMT (A0A0J8C0D9), PGDH (A0A0J8BRE3) and CS (A0A0J8BI86) (Fig. 2; Table 1). Stamen and pollen development is a high-energy-requiring process [5], and the failure of pollen development in CMS lines reflects the abnormal expression of these proteins. Several studies on plant proteomics have also suggested that carbohydrate and energy metabolism is closely related to male plant sterility [37, 52].

Most previous studies showed that the downregulation of genes or proteins associated with carbohydrate and energy metabolism in sterile lines resulted in insufficient energy supply and led to abortion in plants. Similar to the above, two proteins downregulated in the CMS line were also found in this study. In detail, the expression of GAPDH in the CMS line was downregulated compared with that in the restorer line, and its mRNA abundance was significantly lower in CMS than in the maintainer line (Fig. 3a). GAPDH is a key enzyme in carbohydrate metabolism and is involved in the formation of ATP in the glycolytic pathway, DNA repair, tRNA export, and membrane fusion and transport [53]. Furthermore, the association of GAPDH with cell survival may occur by providing ATP to maintain mitochondrial membrane potential via ATPase, helping to counteract the effects of energy collapse by the loss of mitochondrial function [53]. Decreased GAPDH may block the carbohydrate metabolism pathway, resulting in a shortage of energy

supply, which affects anther development. In wolfberry and soybean, GAPDH downregulation in the sterile line led to insufficient energy and sterility, which was consistent with our conclusion [51, 54]. Furthermore, the expression level of PGDH was lower in the CMS line than in the restorer line. PGDH is a member of the oxidoreductase homolog family and plays a role in allosteric regulation [55], which suggests that decreased PGDH would hinder allosteric regulation, resulting in a harmful effect on ATP synthesis. Thus, there may be a direct relationship between the occurrence of CMS and allosteric regulation reduction.

In contrast to previous research, three proteins upregulated in the CMS line that were associated with carbohydrate and energy metabolism were identified in this study. The expression of ATP- $\alpha$  was higher in the CMS line than in the maintainer line according to our iTRAQ and qRT-PCR results (Supplementary Table S1 and Fig. 3). An investigation of the mechanism underlying CMS in kenaf showed that ATP- $\alpha$  and ATP- $\beta$  were differentially expressed in the CMS line [31]. ATP synthase is a key enzyme in the process of oxidative phosphorylation of mitochondria [24] and plays a critical role in energy metabolism. ATP- $\alpha$  and ATP- $\beta$  work together, but the overexpression of ATP- $\alpha$  affects the normal functioning of ATP synthase, suggesting that microspore abortion in the CMS line may be related to abnormal expression of ATP- $\alpha$ . SHMT catalyzes the conversion of glycine to serine and participates in the photorespiration process [56–57]. A previous study in temperature-sensitive wheat reported a decrease in SHMT in the sterile line, which may inhibit photorespiration [58]. However, this finding differed from that of our iTRAQ results, which revealed the different expression patterns of SHMT in different species, but all affected the photorespiration process (Fig. 3). This phenomenon is similar to previous studies, in which CMS-related genes in many crops showed rare similarity to each other, and all led to a similar CMS phenomenon [59]. This implies that common pathways in all kinds of CMS types must exist and be more important than each CMS gene. The TCA cycle is the most important metabolic pathway for energy production under aerobic conditions [60]. CS distributed in mitochondria is a critical enzyme in this cycle. CS catalyzes the reaction of oxaloacetic acid (OAA) and acetyl-CoA to form citric acid and CoA [61]. Surprisingly, both iTRAQ and qRT-PCR (Fig. 3a) revealed that the CS expression level was higher in the CMS line than in the maintainer and restorer lines, which would normally convert more acetyl-CoA into energy. However, CS may not have a regulatory role in those tissues where its activity is in considerable excess of the maximal rates of acetyl-CoA production or isocitrate oxidation [62], which still needs to be further verified.

### 4.3. DEPs involved in binding

Two DEPs related to ion binding and nucleotide binding were identified in this study. Annexin is a  $\text{Ca}^{2+}$ -binding protein that interacts with membrane phospholipids in a calcium-dependent manner [50]. In pepper, the downregulation of annexin in the sterile line disrupted the  $\text{Ca}^{2+}$  balance and reduced fertility [50]. Calcium was established as a second messenger that plays an important role during plant growth and development [52]. In this study, the abundance of annexin (A0A0J8C5G7) in the CMS line was significantly lower than that in the maintainer and restorer lines (Table 2), and there was no difference between the maintainer and restorer lines. These results indicated that downregulation of annexin may be associated with the onset of male infertility. In detail, the downregulation of annexin hindered the calcium-binding process, which impaired  $\text{Ca}^{2+}$  homeostasis;  $\text{Ca}^{2+}$  cannot function properly as a second

messenger and reduced the interaction between annexin and membrane phospholipids. Furthermore, we found that H2A (A0A0J8BEW7) content was lower in the CMS line than in the restorer line. Histone is involved in nucleotide binding and plays an essential role in gene expression control and genome management. Previous studies also reported that the histone content in sterile lines was lower than that in maintainers in wheat and pepper [63–64]. The abnormal expression of H2A may disrupt nucleotide binding and gene expression, which in turn affects anther growth and development and leads to abortion of the plant. Changes in both proteins hinder the binding process, disrupt the balance of the substance during the reaction and cause plant sterility.

## 5. Conclusion

In our research, we used iTRAQ technology to identify a total of 2260 differentially expressed proteins related to the male sterility phenotype involved in protein metabolism, carbohydrate and energy metabolism, and binding from three lines of sugar beets. More specifically, some cysteine and methionine metabolism proteins (A0A0J8BGE0, A0A0J8CZM6, A0A0J8D7W0 and A0A0J8BCR7) may play important roles during the formation of CMS. In addition, we identified 13 key DEGs potentially associated with sugar beet CMS. The way that the proteins associated with carbohydrate and energy metabolism and binding affect male sterility was further elucidated. It will be interesting to study the mutants associated with CMS proteins to better understand the molecular mechanisms of CMS in the future.

## Abbreviations

60S ribosomal protein L36 (L36); Aspartate aminotransferase (AAT); ATP synthase subunit  $\alpha$  (ATP- $\alpha$ ); Chalcone-flavanone isomerase family protein (CHI 2-A); Citrate synthase (CS); Cytoplasmic male sterility (CMS); D-3-phosphoglycerate dehydrogenase (PGDH); Differentially expressed proteins (DEPs); Glutamine synthetase (GS); Glutathione synthetase (GSH-S); Cysteine synthase (Cs); Glyceraldehyde-3-phosphate dehydrogenase (GAPDH); Histone 2A (H2A); Isobaric tag for relative and absolute quantitation technology (iTRAQ); Quantitative real-time polymerase chain reaction (qRT-PCR); Serine hydroxymethyltransferase (SHMT); Superoxide dismutase (SOD); Glutamate-cysteine ligase (GCL); Glutathione (GSH); Programmed cell death (PCD)

## Declarations

### Compliance with Ethical Standards:

Funding: This study was funded by National Natural Science Foundation of China (31271781).

Ethical approval: This article does not contain any studies with human participants or animals performed by any of the authors.

# References

1. Mihr C, Baumgärtner M, Dieterich JH et al (2001) Proteomic approach for investigation of cytoplasmic male sterility (CMS) in Brassica. *J Plant Physiol* 158:787–794
2. Sun QP, Hu CF, Hu J et al (2009) Quantitative proteomic analysis of CMS-related changes in Honglian CMS rice anther. *Protein J* 28:341–348
3. Laser KD, Lersten NR (1972) Anatomy and cytology of microsporogenesis in cytoplasmic male sterile angiosperms. *Bot Rev* 38:425–454
4. Chase CD (2007) Cytoplasmic male sterility: a window to the world of plant mitochondrial-nuclear interactions. *Trends Genet* 23:81–90
5. Schnable PS, Wise RP (1998) The molecular basis of cytoplasmic male sterility and fertility restoration. *Trends Plant Sci* 3:175–180
6. Hanson MR, Bentolila S (2004) Interactions of mitochondrial and nuclear genes that affect male gametophyte development. *Plant Cell* 16:154–169
7. Yamamoto MP, Shinada H, Onodera Y, Komaki C, Mikami T, Kubo T (2008) A male sterility-associated mitochondrial protein in wild beets causes pollen disruption in transgenic plants. *Plant J* 54:1027–1036
8. Hussy I, Hawkes FR (2005) Continuous hydrogen production from sucrose and sugarbeet. *Int J Hydrogen Energy* 30:471–483
9. Owen FV (1945) Cytoplasmically inherited male-sterility in sugar beets. *J Agric Res* 71:423–440
10. Kubo T, Nishizawa S, Sugawara A, Itchoda N, Estiati A, Mikami T (2000) The complete nucleotide sequence of the mitochondrial genome of sugar beet (*Beta vulgaris* L.) reveals a novel gene for tRNACys (GCA). *Nucleic Acids Res* 28:2571–2576
11. Satoh M, Kubo T, Nishizawa S, Estiati A, Itchoda N, Mikami T (2004) The cytoplasmic male-sterile type and normal type mitochondrial genomes of sugar beet share the same complement of genes of known function but differ in the content of expressed ORFs. *Mol Gen Genomics* 272:247–256
12. Duchenne M, Lejeune B, Fouillard P, Quetier F (1989) Comparison of the organization and expression of mtDNA of fertile and male-sterile sugar beet varieties (*Beta vulgaris* L.). *Theor. Appl Genet* 78:633–640
13. Dudareva NA, Popovsky AV, Kasjanova UV, Veprev SG, Mglinets AV, Salganik RI (1991) Expression of mitochondrial genes in fertile and sterile sugar beet cytoplasms with different nuclear fertility restorer genes. *Theor Appl Genet* 83:217–224
14. Senda M, Harada T, Mikami T, Sugiura M, Kinoshita T (1991) Genomic organization and sequence analysis of the cytochrome oxidase subunit II gene from normal and male-sterile mitochondria in sugar beet. *Curr Genet* 19:175–181
15. Xue Y, Collin S, Davies DR, Thomas CM (1994) Differential screening of mitochondrial cDNA libraries from male-fertile and cytoplasmic male-sterile sugar-beet reveals genome rearrangements at *atp6* and *atpA* loci. *Plant Mol Biol* 25:91–103

16. Yamamoto MP, Kubo T, Mikami T (2005) The 5'-leader sequence of sugar beet mitochondrial atp6 encodes a novel polypeptide that is characteristic of Owen cytoplasmic male sterility. *Mol Gen Genomics* 273:342–349
17. Halldén C, Lind C, Møller IM (1992) Variation in mitochondrial translation products in fertile and cytoplasmic male-sterile sugar beets. *Theor Appl Genet* 85:139–145
18. Wesołowski W, Szklarczyk M, Zalonek M et al (2015) Analysis of the mitochondrial proteome in cytoplasmic male-sterile and male-fertile beets. *J Proteomics* 119:61–74
19. Komatsu S (2005) Rice Proteome Database: a step towards functional analysis of the rice genome. *Plant Mol Biol* 59:179–190
20. Wang S, Zhang G, Zhang Y et al (2015) Comparative studies of mitochondrial proteomics reveal an intimate protein network of male sterility in wheat (*Triticum aestivum* L.). *J Exp Bot* 66:6191–6203
21. Huang L, Xiang J, Liu J, Rong T, Wang J, Lu Y, Tang Q et al (2012) Expression characterization of genes for CMS-C in maize. *Protoplasma* 249:1119–1127
22. Dewey RE, Timothy DH, Levings CS (1987) A mitochondrial protein associated with cytoplasmic male sterility in the T cytoplasm of maize. *Proc. Natl. Acad. Sci. USA* 84:5374-5378
23. Zhang WJ, Li CZ, Huang HQ, Wang ZY, Peng YK (2007) Different proteins in mitochondrial proteome of T-type maize cytoplasmic male-sterile line and its maintainer line. *J Mol Cell Biol* 40:410–418
24. Sheoran IS, Sawhney VK (2010) Proteome analysis of the normal and Ogura (ogu) CMS anthers of *Brassica napus* to identify proteins associated with male sterility. *Botany* 88:217–230
25. Sheoran IS, Ross ARS, Olson DJH, Sawhney VK (2009) Differential expression of proteins in the wild type and 7B-1 male-sterile mutant anthers of tomato (*Solanum lycopersicum*): a proteomic analysis. *J Proteome* 71:624–636
26. Bonner WD Jr (1967) A general method for the preparation of plant mitochondria. *Methods Enzymol* 10:3–7
27. Nagahashi J, Hiraike K (1982) Effects of centrifugal force and centrifugation time on the sedimentation of plant organelles. *Plant Physiol* 69:546–548
28. Lind C, Halldén C, Møller IM (1991) Protein synthesis in mitochondria purified from roots, leaves and flowers of sugar beet. *Physiol Plant* 83:7–16
29. Douce R, Bourguignon J, Brouquisse R, Neuburger M (1987) Isolation of plant mitochondria: General principles and criteria of integrity. *Methods Enzymol* 148:403–415
30. Gupta KJ, Stoimenova M, Kaiser WM (2005) In higher plants, only root mitochondria, but not leaf mitochondria reduce nitrite to NO, in vitro and in situ. *J Exp Bot* 56:2601–2609
31. Chen P, Liao J, Huang Z et al (2014) Comparative proteomics study on anther mitochondria between cytoplasmic male sterility line and its maintainer in Kenaf (*Hibiscus cannabinus* L.). *Crop Sci* 54:1103–1114
32. Jia D, Wang B, Li X et al (2017) Proteomic analysis revealed the fruiting-body protein profile of *Auricularia polytricha*. *Curr Microbiol* 74:943–951

33. Hu X, Li N, Wu L et al (2015) Quantitative iTRAQ-based proteomic analysis of phosphoproteins and ABA-regulated phosphoproteins in maize leaves under osmotic stress. *Sci Rep* 5:15626
34. Sandberg A, Lindell G, Källström BN et al (2012) Tumor proteomics by multivariate analysis on individual pathway data for characterization of vulvar cancer phenotypes. *Mol Cell Proteomics* 11:M112016998
35. Pin PA, Benlloch R, Bonnet D et al (2010) An antagonistic pair of FT Homologs mediates the control of flowering time in sugar beet. *Science* 330:1397–1400
36. Zheng B, Fang Y, Pan Z et al (2014) iTRAQ-Based quantitative proteomics analysis revealed alterations of carbohydrate metabolism pathways and mitochondrial proteins in a male sterile Cybrid Pummelo. *J Proteome Res* 13:2998–3015
37. Liu J, Pang C, Wei H et al (2015) iTRAQ-facilitated proteomic profiling of anthers from a photosensitive male sterile mutant and wild-type cotton (*Gossypium hirsutum* L.). *J Proteomics* 126:68–81
38. Kirsch JF, Eichele G, Ford GC et al (1984) Mechanism of action of aspartate aminotransferase proposed on the basis of its spatial structure. *J Mol Biol* 174:497–525
39. Gechev TS, Gadjev IZ, Hille J (2004) An extensive microarray analysis of AAL-toxin-induced cell death in *Arabidopsis thaliana* brings new insights into the complexity of programmed cell death in plants. *Cell Mol Life Sci* 61:1185–1197
40. Chambers DA, Imrey PB, Cohen RL et al (1991) A longitudinal study of aspartate aminotransferase in human gingival crevicular fluid. *J periodontal res* 26:65–74
41. Dangl JL, Jones JDG (2001) Plant pathogens and integrated defence responses to infection. *Nature* 411:826–833
42. Kuriyama H, Fukuda H (2002) Developmental programmed cell death in plants. *Curr Opin Plant Biol* 5:568–573
43. Yang Y, Dieter MZ, Chen Y et al (2002) Initial characterization of the glutamate-cysteine ligase modifier subunit *gclm* (-/-) knockout mouse. *J Biol Chem* 277:49446–49452
44. Turton HE, Dawes IW, Grant CM (1997) *Saccharomyces cerevisiae* exhibits a yAP-1-mediated adaptive response to malondialdehyde. *J Bacteriol* 179:1096–1101
45. Grant CM, MacIver FH, Dawes IW (1997) Glutathione synthetase is dispensable for growth under both normal and oxidative stress conditions in the yeast *Saccharomyces cerevisiae* due to an accumulation of the dipeptide gamma-glutamylcysteine. *Mol Biol Cell* 8:1699–1707
46. Droux M (2004) Sulfur assimilation and the role of sulfur in plant metabolism: a survey. *Photosynth Res* 79:331–348
47. Hell R, Jost R, Berkowitz O, Wirtz M (2002) Molecular and biochemical analysis of the enzymes of cysteine biosynthesis in the plant *Arabidopsis thaliana*. *Amino Acids* 22:245–257
48. Wirtz M, Hell R (2006) Functional analysis of the cysteine synthase protein complex from plants: Structural, biochemical and regulatory properties. *J Plant Physiol* 163:273–286

49. Mifflin BJ, Habash DZ (2002) The role of glutamine synthetase and glutamate dehydrogenase in nitrogen assimilation and possibilities for improvement in the nitrogen utilization of crops. *J Exp Bot* 53:979–987
50. Wu Z, Cheng J, Qin C et al (2013) Differential proteomic analysis of anthers between cytoplasmic male sterile and maintainer lines in *Capsicum annuum* L. *Int J Mol Sci* 14:22982–22996
51. Zheng R, Yue S, Xu X et al (2012) Proteome analysis of the wild and YX-1 male sterile mutant anthers of Wolfberry (*Lycium barbarum* L.). *PLoS ONE* 7:e41861
52. Yan J, Tian H, Wang S et al (2014) Pollen developmental defects in ZD-CMS rice line explored by cytological, molecular and proteomic approaches. *J Proteomics* 108:110–123
53. Tristan C, Shahani N, Sedlak TW, Sawa A (2011) The diverse functions of GAPDH: Views from different subcellular compartments. *Cell Signal* 23:317–323
54. Li J, Ding X, Han S et al (2016) Differential proteomics analysis to identify proteins and pathways associated with male sterility of soybean using iTRAQ-based strategy. *J Proteomics* 138:72–82
55. Grant GA, Schuller DJ, Banaszak LJ (1996) A model for the regulation of D-3-phosphoglycerate dehydrogenase, a Vmax-type allosteric enzyme. *Protein Sci* 5:34–41
56. Somerville CR, Ogren WL (1981) Photorespiration-deficient mutants of *Arabidopsis thaliana* lacking mitochondrial serine transhydroxymethylase activity. *Plant Physiol* 67:666–671
57. Moreno JI, Martin R, Castresana C et al (2005) A serine hydroxymethyltransferase that functions in the photorespiratory pathway influences resistance to biotic and abiotic stress. *Plant J* 41:451–463
58. Li YY, Li Y, Fu QG et al (2015) Anther proteomic characterization in temperature sensitive Bainong male sterile wheat. *Biol Plant* 59:273–282
59. Linke B, Börner T (2005) Mitochondrial effects on flower and pollen development. *Mitochondrion* 5:389–402
60. Alp PR, Newsholme EA, Zammit VA (1976) Activities of citrate synthase and NAD<sup>+</sup>-linked and NADP<sup>+</sup>-linked isocitrate dehydrogenase in muscle from vertebrates and invertebrates. *Biochem J* 154:689–700
61. Jakob U, Lilie H, Meyer I, Buchner J (1995) Transient interaction of Hsp90 with early unfolding intermediates of citrate synthase. *J Biol Chem* 270:7288–7294
62. Shepherd D, Garland PB (1969) Citrate synthase from rat liver: [EC 4.1.3.7 Citrate oxaloacetate-lyase (CoA-acetylating)]. *Methods Enzymol* 13:11–16
63. Zhang X, Chen B, Zhang L et al (2015) Identification of proteins associated with cytoplasmic male sterility in pepper (*Capsicum annuum* L.). *S. Afr. J Bot* 100:1–6
64. Jain AK, Rathore RKS, Chauhan SVS et al (1982) Histochemical studies in some cytoplasmic male sterile lines of wheat. *Fac Agr Hokkaido Univ* 61:143–149

## Figures

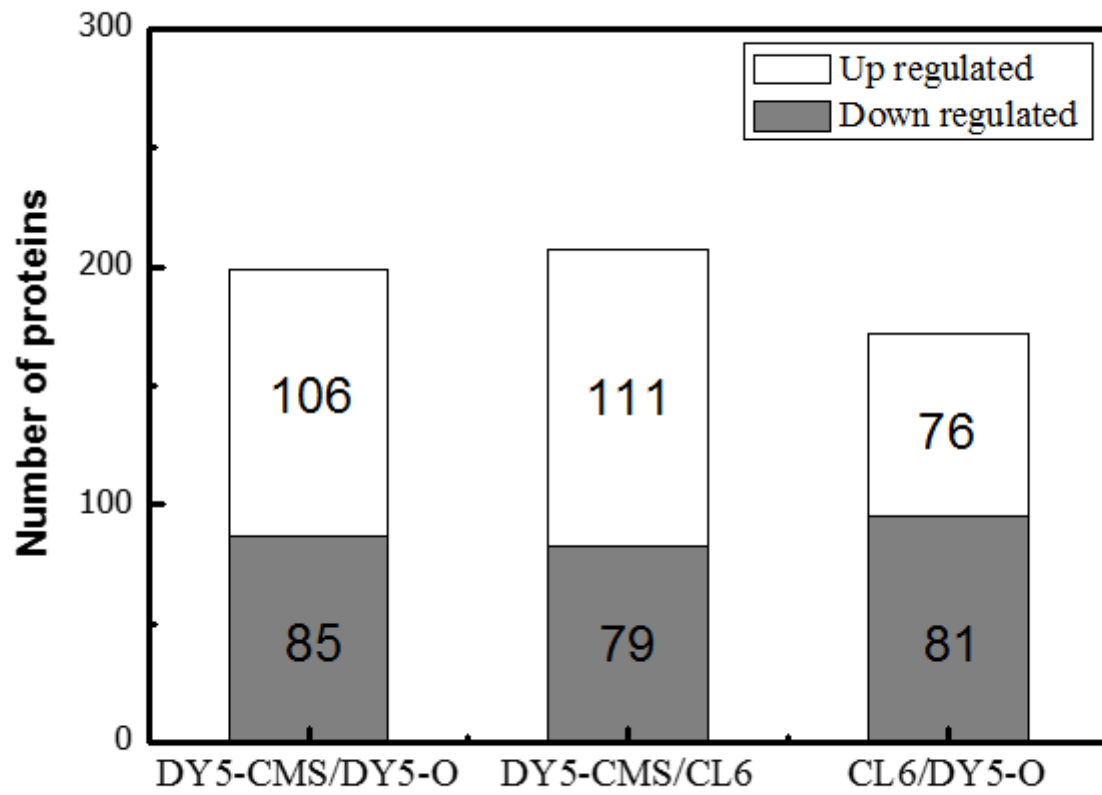


**Figure 1**

Number of up- or downregulated proteins in different comparisons. DY5-CMS, sterile line; DY5-O, maintainer line; CL6, fertility restorer line.

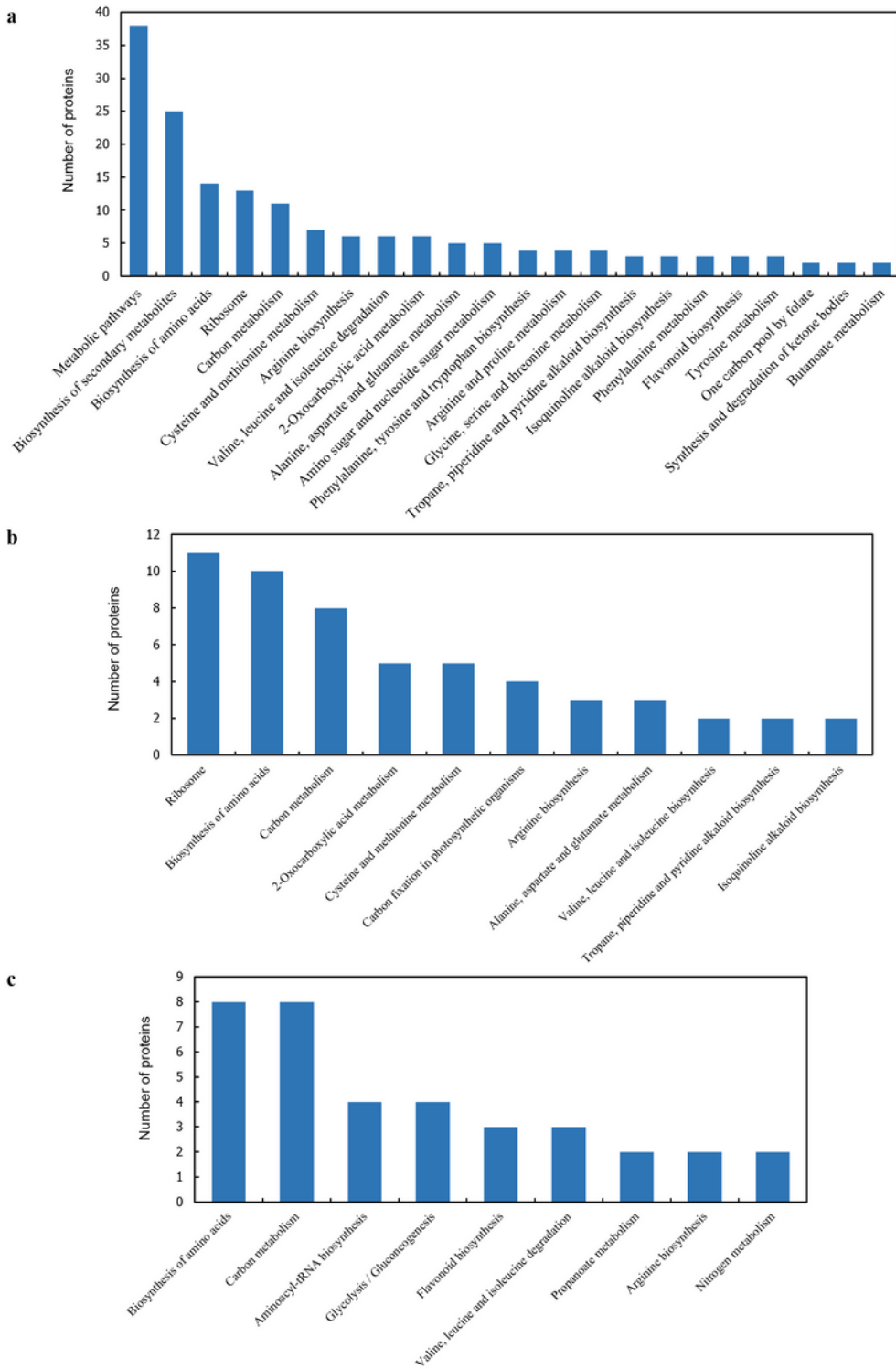


**Figure 2**

Distribution of significantly enriched KEGG pathways of DEPs from DY5-CMS/DY5-O (a), DY5-CMS/CL6 (b) and CL6/DY5-O (c). DY5-CMS, sterile line; DY5-O, maintainer line; CL6, fertility restorer line.

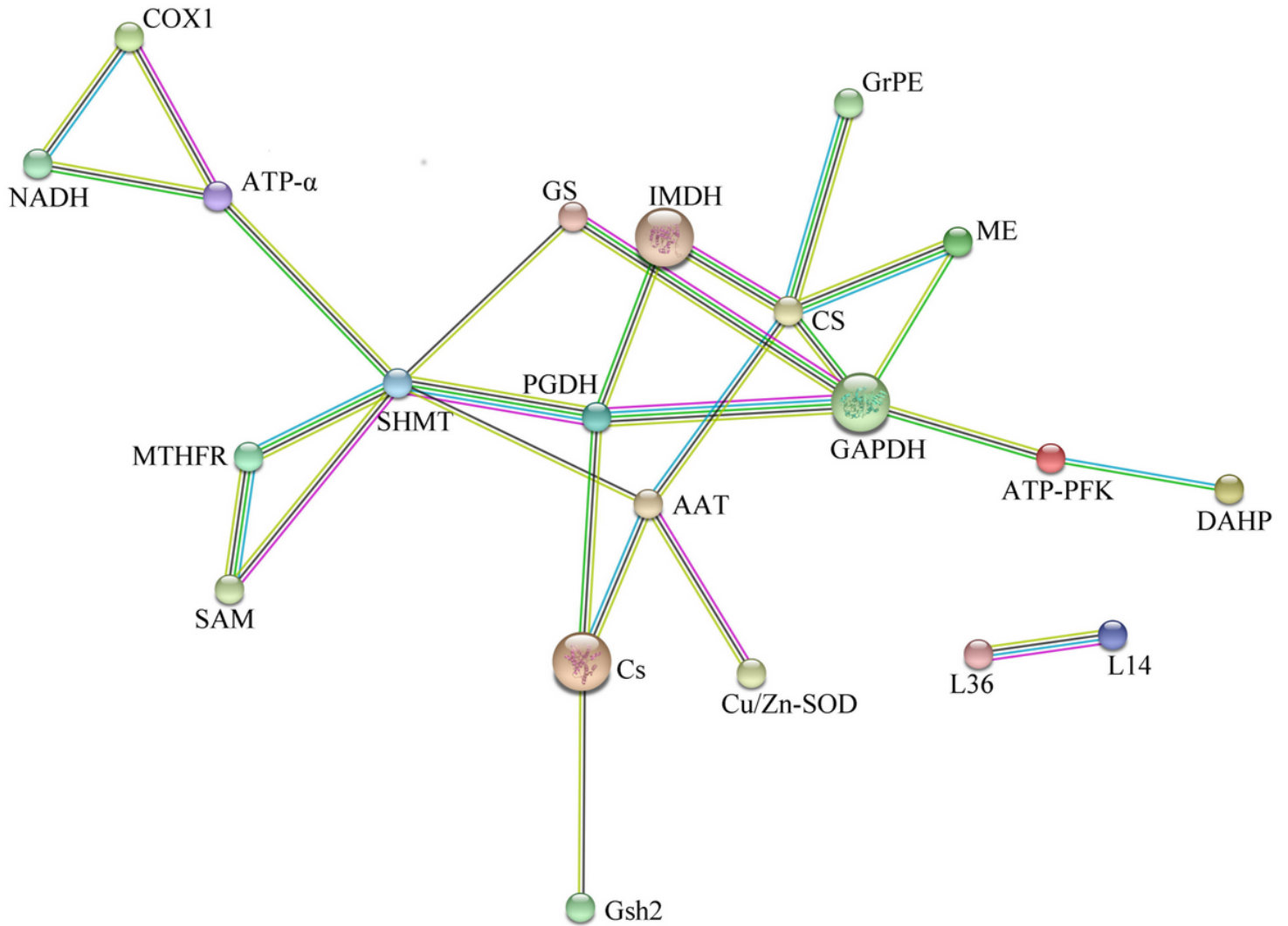


**Figure 3**

Interaction network analysis of DEPs (from the comparisons DY5-CMS/DY5-0, DY5-CMS/CL6 and CL6/DY5-0). The interaction network was analyzed by STRING software (<http://string-db.org>). In this network, the lines represent functional associations between proteins, and the thickness of the lines represents the level of confidence in association reported.

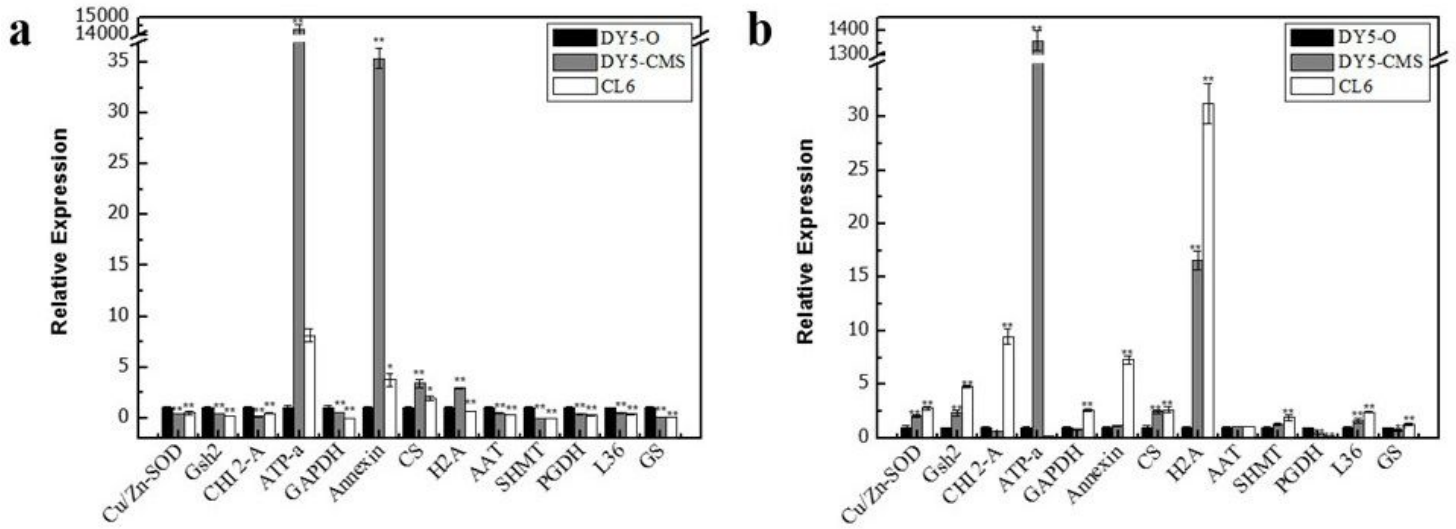


**Figure 4**

Gene expression analysis by qRT-PCR (using RNA extracted from roots (a) and leaves (b), respectively). DY5-CMS, sterile line; DY5-O, maintainer line; CL6, fertility restorer line.

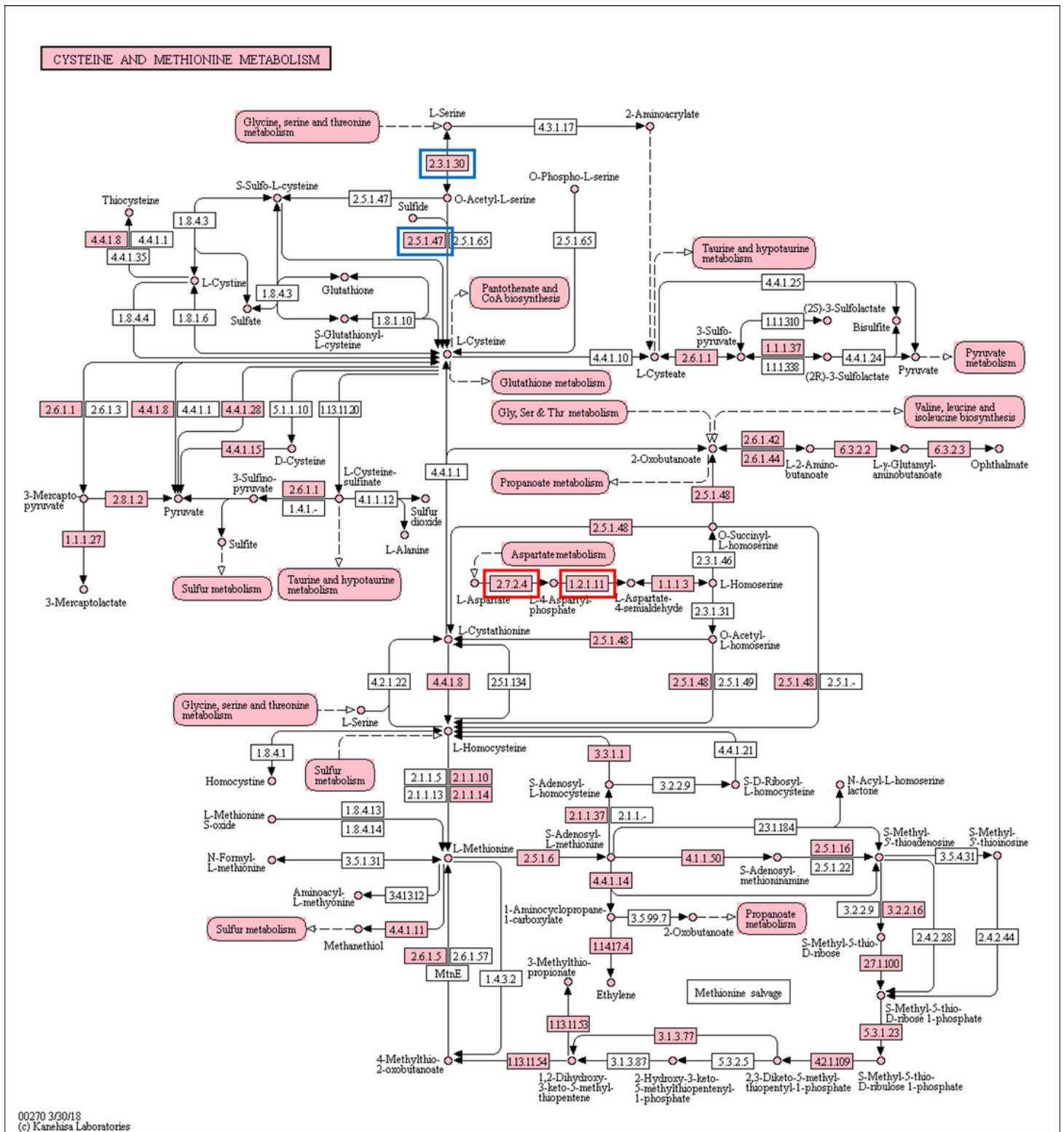


**Figure 5**

Identified proteins involved in the cysteine and methionine metabolism in sugar beet. The red box represents AOA0J8BGE0 and AOA0J8CZM6; The blue box represents AOA0J8D7W0; and the pink box represents AOA0J8D7W0.

## Supplementary Files

This is a list of supplementary files associated with this preprint. Click to download.

- [SupplementaryMaterialIntroduction.docx](#)
- [SupplementalTableS1.xlsx](#)
- [SupplementalTableS2.xlsx](#)
- [SupplementalTableS3.xlsx](#)